

12-16 July 2015, Bellevue, WA

# Sub-GLE Solar Particle Events and the Implications for Lightly-Shielded Systems Flown During an Era of Low Solar Activity

William Atwell

*Retired Boeing Technical Fellow, Boeing Research & Technology, Houston, TX 77059 USA*

Allan J. Tylka

*NASA Goddard Spaceflight Center, Greenbelt, MD 20771 USA*

William Dietrich

*Consultant, Prospect Heights, IL 60070 USA*

Kristina Rojdev

*NASA Johnson Space Center, Houston, TX 77059 USA*

Courtney Matzkind

*Boeing Research & Technology, Houston, TX 77059 USA*

Many of the large space missions must be very rigorous in their designs to reduce risk from radiation damage as much as possible. Some ways of reducing this risk have been to build in multiple redundancies, purchase/develop radiation hardened electronics parts, and plan for worst case radiation environment scenarios. These methods work well for these ambitious missions that can afford the costs associated with these meticulous efforts. However, there have been more small spacecraft and CubeSats with smaller duration missions entering the space arena, which can take some additional risks, but cannot afford to implement all of these risk-reducing methods. Therefore, one way to quantify the radiation exposure risk for these smaller spacecraft would be to investigate the radiation environment pertinent to the mission to better understand these radiation exposures, rather than always designing to the infrequent, worst-case environment. In this study, we have investigated 34 historical solar particle events (1974-2010) that occurred during a time period when the sun spot number (SSN) was less than 30. These events contain Ground Level Events (GLE), sub-GLEs, and sub-sub-GLEs<sup>1-3</sup>. GLEs are extremely energetic solar particle events (SPEs) having proton energies often extending into the several GeV range and producing secondary particles in the atmosphere, mostly neutrons, observed with ground station neutron monitors. Sub-GLE events are less energetic, extending into the several hundred MeV range, but without producing detectable levels of secondary atmospheric particles. Sub-sub GLEs are even less energetic with an observable increase in protons at energies greater than 30 MeV, but no observable proton flux above 300 MeV. The spectra for these events were fitted using a double power law fit in particle rigidity, called the Band fit method (Tylka and Dietrich, 2009). The differential spectra were then input into the NASA Langley Research Center HZETRN 2005 (F. F. Badavi, 2006), which is a high-energy particle transport/dose code, to determine the dose in various thicknesses of aluminum, representing the spacecraft. This paper will detail the absorbed dose results of each of these environments, as well as analyze the data to better understand the doses over small thicknesses that are more relevant to small spacecraft and satellites, such as CubeSats. In addition, we will discuss the implications of these data and provide some recommendations that may be useful to spacecraft designers of these smaller spacecraft/CubeSat-type missions.

## Nomenclature

<i>Al</i>	= chemical symbol for aluminum
<i>cGy</i>	= absorbed dose unit centiGray
<i>CPME</i>	= Johns Hopkins University Applied Physics Laboratory's Charged Particle Measurement Experiment
<i>CRNE</i>	= University of Chicago's Cosmic Ray Nuclei Explorer
<i>EPEAD</i>	= Energetic Proton, Electron, and Alpha Detectors; successor to the EPS on the GOES satellite
<i>EPS</i>	= Energetic Particle Sensors on the GOES satellite
<i>GLE</i>	= ground level event (or enhancement)
<i>GME</i>	= Goddard Medium Energy Experiment
<i>GOES</i>	= Geostationary Operational Environmental Satellite
<i>HDPE</i>	= high density polyethylene
<i>HEPAD</i>	= High Energy Particle Detector, which measures protons above 330 MeV on the GOES satellite
<i>HZETRN</i>	= NASA Langley Research Center-developed high energy particle transport/dose code
<i>IMP8</i>	= Interplanetary Monitoring Platform satellite 8
<i>NASA</i>	= National Aeronautics and Space Administration
<i>NGDC</i>	= National Geophysical Data Center within NOAA Boulder
<i>NM</i>	= neutron monitor
<i>NOAA</i>	= National Oceanic and Atmospheric Administration in Boulder, CO
<i>SEP</i>	= solar energetic particle
<i>SPE</i>	= solar proton event
<i>SSN</i>	= smoothed sunspot number
<i>TID</i>	= total ionizing dose

## I. Introduction

**S**OLAR proton events represent the single most greatest threat for acute radiation exposure. For human spaceflight missions and long duration, discovery class, deep space missions, mitigating this radiation risk is extremely important to the mission. Thus, the mission designers typically take a worst-case scenario approach when designing their vehicles. This design approach leads to increased shielding mass in the form of storm shelters for humans (increased launch costs) and high cost testing of electronics to verify that they will survive the worst-case radiation environments.

Due to recent budget restrictions, having multiple large scale missions is not feasible anymore, and smaller, short-duration, higher-risk missions are becoming the normal operating procedure for spaceflight in general. At NASA, these types of missions are rated Class D and are precursors for larger missions later on. Their purpose is to perform science and test out new technology developments that are necessary for these future missions. Outside of NASA, several commercial companies and universities have started experimenting with small spacecraft, such as CubeSats and NanoSats. These spacecraft tend to be relatively small and inexpensive, and the mission durations can be very short, on the order of weeks. Thus, these spacecraft can generally accept a greater amount of risk in their designs.

If these spacecraft use the typical method of designing to the worst-case radiation environment, they may be overdesigning their spacecraft and accepting an unnecessary increase in mass and cost. Furthermore, the sun has recently entered a relatively quiet timeperiod, unprecedented in the manned spaceflight era. Solar physicists are predicting that the sun will remain relatively inactive for several years to come. Thus, it is important to reexamine the methods used in determining radiation mitigation necessary for these newer types of missions.

In this study, we examine the quiet solar environment, with sunspot numbers less than 30 in the historical record. We focus on SPEs in this time period and evaluate the dose to spacecraft over a range of thicknesses. We then discuss the implications of this data for designers of these smaller spacecraft and shorter duration missions.

## II. Background

The deep space radiation environment is made up of two primary sources of radiation: solar particle events (SPEs) from the sun and galactic cosmic rays (GCRs) from outside the solar system. For this study, we are focusing only on SPEs, and particularly those SPEs that occur when the sun has a smoothed sunspot number (SSN) less than 30 (SSN data provided by . The SSN serves as a general measure of solar activity, for which we have a 250 year historical

record. The sun follows an approximately eleven year cycle in which it goes through a period of maximum activity and a period of minimum activity, as denoted by the SSN (Figure 1). Figure 1 shows the sunspot numbers for each of the solar cycles in the manned space era (since 1964). One thing to note in Figure 1 is that the current solar cycle, number 24, has significantly lower sun spot numbers than any other cycle of the manned spaceflight era.

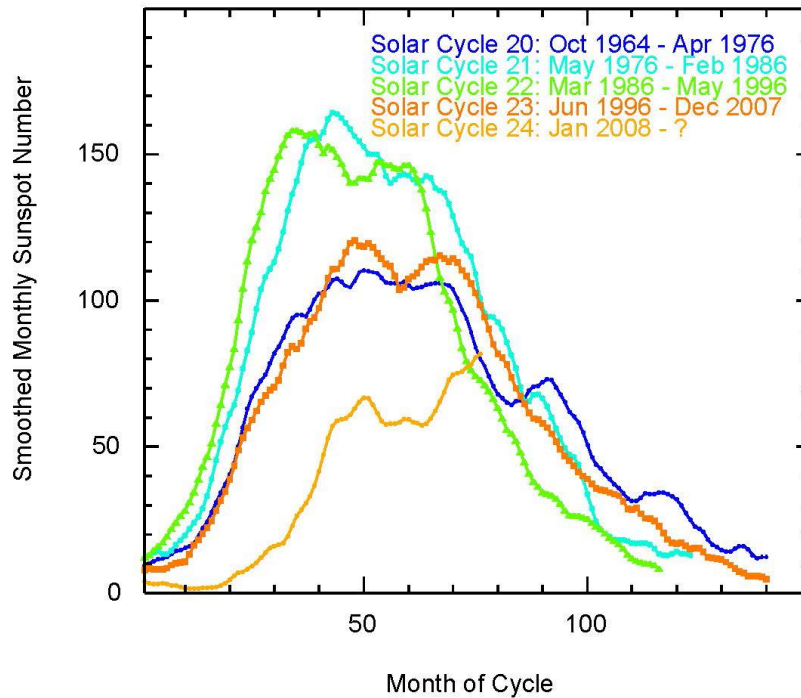
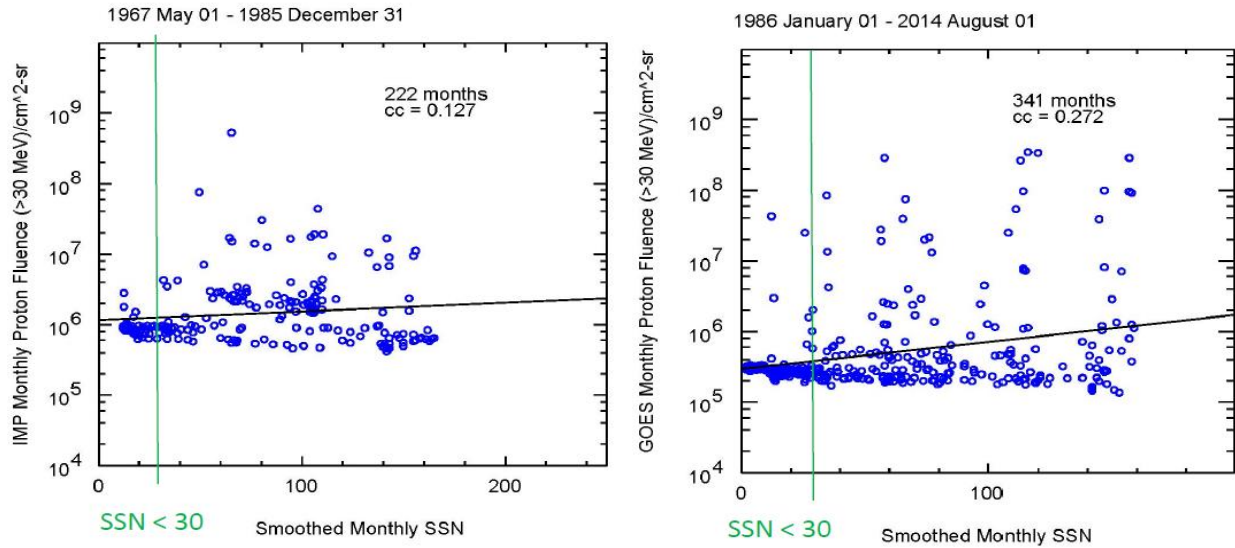


**Figure 1: Smoothed sunspot numbers in the manned space era (since 1964) plotted versus the month of the Cycle (for Solar Cycles 20-24).**

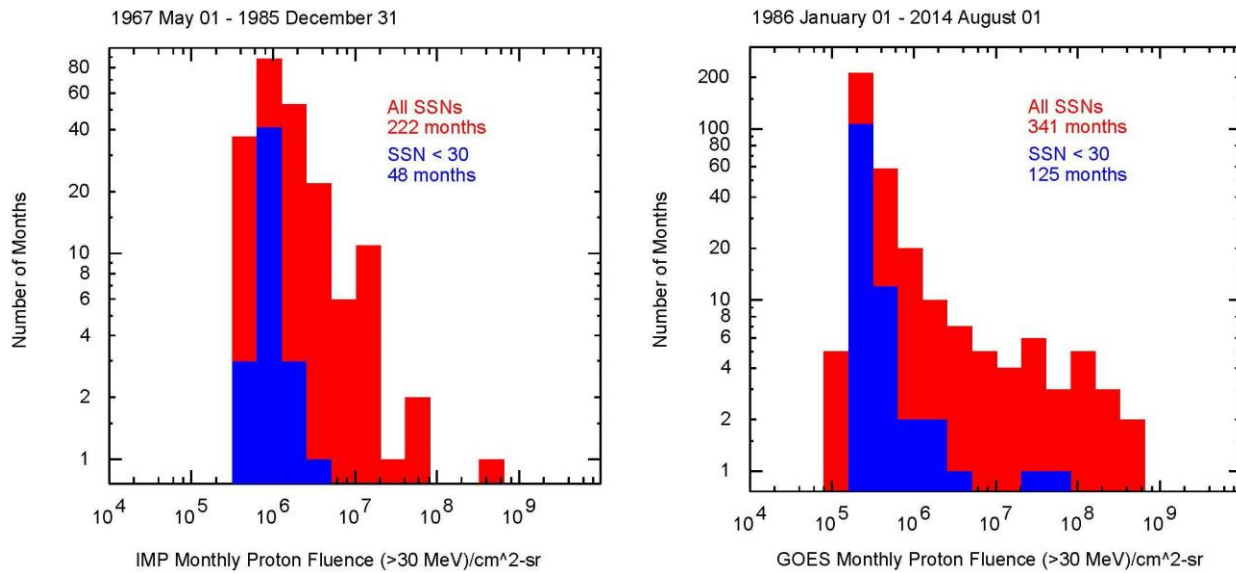
To better understand the implications of the low sunspot numbers for cycle 24, we plotted historical data of the monthly-accumulated >30 MeV proton fluence as a function of SSN from 1967 to 2014 (

Figure 2; SSNs provided by provided by WDC-SILSO, Royal Observatory of Belgium, Brussels ). In general, these data shows that the solar energetic particle (SEP) production is not strongly correlated with SSN. Nevertheless, when considering those months with SSN < 30, the largest monthly fluence values are absent (

Figure 3). Thus, designing to a worst case SPE scenarios, which tends to occur during periods of high SSN, it would be a very conservative approach for missions to be flown in an era of comparatively low solar activity.



**Figure 2: The monthly proton fluence as a function of sun spot number. The image on the left has data from the IMP instrument and is from May 1967-December 1985. The image on the right is from the GOES instrument and is from January 1986 to August 2014.**



**Figure 3: The number of months with a particular proton fluence at energies greater than 30 MeV.**

### III. Data Sources and Analysis Methods

Thirty-four solar proton events that occurred during the 1974-2010 time period when the SSN was less than 30 were identified and selected for analysis. Table 1 shows the four Band fit parameters for each event.

**Table 1: Band fit parameters for the 34 solar proton events.**

Yr	Mo	Day	$J_0$ (p/cm <sup>2</sup> )	$\gamma_1$	$\gamma_2$	$R_0$ (GV)
<u>GLEs</u>						
1976	Apr	30	7.620E+06	1.710	6.33	0.2054
2006	Dec	13	1.330E+08	1.045	5.80	0.1765
<u>sub-GLEs</u>						
1974	Nov	05	1.182E+06	1.705	7.01	0.1390
1975	Aug	21	8.016E+05	0.958	8.83	0.1035
1975	Aug	22	4.376E+06	0.605	5.74	0.0978
1976	Aug	22	2.853E+06	1.182	9.03	0.0877
1985	Jan	22	3.090E+06	1.079	9.23	0.0952
1985	Apr	24	2.402E+04	4.076	6.83	0.3641
1985	Jul	09	2.362E+06	1.506	7.80	0.1140
1985	Jul	17	2.612E+06	-0.094	4.35	0.1627
1986	Feb	06	1.163E+07	1.030	10.20	0.1425
1986	Feb	07	1.055E+06	2.753	8.48	0.1553
1986	Feb	14	4.699E+05	3.358	8.58	0.1531
1994	Oct	19	1.009E+05	2.787	5.02	0.1607
2005	Jun	16	2.035E+08	-0.187	4.36	0.0839
2005	Sep	07	5.949E+06	3.098	5.55	0.3171
2006	Dec	05	4.178E+07	2.320	8.97	0.1697
<u>sub-sub</u>						
1986	Feb	04	1.288E+06	0.684	5.33	0.0847
1986	Feb	10	3.579E+05	1.140	4.70	0.1177
1986	Feb	16	1.881E+06	1.681	7.37	0.0697
1986	Mar	06	1.407E+05	2.296	6.54	0.0949
1986	May	04	3.785E+06	0.714	4.74	0.0945
2005	May	13	3.693E+10	0.504	6.15	0.0181
2005	May	14	1.680E+11	0.303	8.76	0.0191
2005	Jul	13	2.850E+07	0.790	7.13	0.0404
2005	Jul	14	1.596E+11	-1.258	9.69	0.0309
2005	Jul	17	1.072E+08	0.496	7.39	0.0500
2005	Jul	25	4.710E+08	0.815	7.72	0.0464
2005	Aug	22	1.380E+10	0.078	9.03	0.0350
2005	Sep	01	5.555E+06	-0.306	3.51	0.1189
2005	Sep	13	3.318E+10	-0.298	9.47	0.0306
2006	Jul	06	1.767E+06	0.896	4.92	0.0771
2006	Dec	14	2.236E+08	0.120	4.67	0.0674
2010	Aug	14	3.179E+06	1.053	5.34	0.0619

In this study, solar energetic proton measurements below 500 MeV came primarily from the IMP8 and GOES satellites. IMP8 had three instruments that monitored solar protons: the Goddard Medium Energy Experiment (GME) from the NASA (McGuire, von Roseninge, & McDonald 1986); the University of Chicago's Cosmic Ray Nuclei

Explorer (CRNE; Garcia-Munoz, Mason, & Simpson 1975; Novikova et al. 2010), and the Johns Hopkins University Applied Physics Laboratory's Charged Particle Measurement Experiment (CPME; Krimigis, Armstrong, & Kohl 1973). The various GOES satellites carried the Energetic Particle Sensors (EPS; Onsager et al. 1996) and its successor, the Energetic Proton, Electron, and Alpha Detectors (EPEAD), (Rodriguez et al. 2010). EPS and EPEAD measured solar protons starting at a few MeV. GOES satellites also carried the High Energy Particle Detector (HEPAD; Sauer 1993), which measures protons above 330 MeV. The GOES, CPME, and GME data were obtained from their respective websites. GOES data were provided by <http://www.ngdc.noaa.gov/stp/satellite/goes/dataaccess.html>; the CPME and GME data were provided by NASA's Omniweb (<http://omniweb.gsfc.nasa.gov/ow.html>) and CDAWeb ([http://cdaweb.sci.gsfc.nasa.gov/cdaweb/sp\\_phys/sites](http://cdaweb.sci.gsfc.nasa.gov/cdaweb/sp_phys/sites)) websites, respectively. One of us (WFD) provided the fully corrected CRNE data.

IMP8 operated between November 1973 and October 2001; fully-corrected GOES proton data are available from January 1986 onward. Thus, data before 1986 come only from IMP8; data after October 2001 come only from GOES. In the intermediate period we have data from both satellites, allowing for independent cross-checks on the results. These cross-checks are particularly valuable in that the instruments have complementary strengths and weaknesses, as discussed below. However, in some events in 1986-2001, in which IMP8 data had severe telemetry gaps, only GOES data were useable.

Two of the events (1976 April 30 and 2006 December 13; Tylka & Dietrich 2010) are so-called Ground-Level Events (GLEs), which had sufficient intensities of protons above ~430 MeV to register in terrestrial neutron monitors (NMs). Details of our methods for extracting event-integrated proton fluences from the world-wide neutron monitor network have been published elsewhere (Tylka & Dietrich 2009). Since each neutron monitor responds to the proton fluence above its local geomagnetic or atmospheric cutoff, it is natural to analyze the NM data as integral fluence in rigidity,  $J(>R)$ , where  $J$  is the event-integrated fluence (in protons/cm<sup>2</sup>) of protons with rigidities greater  $R$ .

Since the NM data were analyzed in terms of  $J(>R)$ , it is convenient to handle the satellite data in the same way. Both GOES and the IMP8/CPME report integral proton fluences. The GME and CRNE data, which are reported as differential fluences (protons/cm<sup>2</sup>-MeV) at various energies, are also easily re-expressed in terms of integral fluences by straight-forward numerical summation. The CRNE instrument reports proton intensities in eight differential channels (from 10.8-95.0 MeV, or equivalently, 0.142-0.431 GV) with the upper-edge of one energy bin corresponding to the lower-edge of the next, without energy gaps. CRNE also reports an integral channel above 95 MeV (0.431 GV). The GME instrument has better energy resolution, with 30 differential bins between 0.88 and 485 MeV, with only one pair of overlapping bins (from different instrument apertures), one small energy gap at 81-87 MeV that is easily bridged by interpolation. Power-law fits to the highest-energy GME channels provide an estimate of the unobserved fluence above 485 MeV. Adding this estimate to sums of the differential channels allows the GME data to be rebinned into 28 integral channels, with thresholds ranging from 0.041 to 0.846 GV.

The designs of the GOES EPS and EPEAD instruments are intended to make them essentially dead-time free, so that they can operate even in the highest-rate environments. High rates in the anti-coincidence shield around the CRNE telescope introduce dead-times in the differential channels. By comparing GOES/EPS and IMP8/CRNE, we have developed methods for deducing a global dead-time correction for the CRNE differential channels as a function of the simultaneously-observed anticoincidence-shield rate (Tylka & Dietrich 1999). Dead-times in the CRNE >95 MeV integral channel are negligible, since the trigger logic for this channel did not include the anti-coincidence shield.

We have found that the GME proton fluxes above 95 MeV are systematically smaller than those from CRNE. For the events in this study, the multiplicative factor needed to bring the GME >95 MeV fluences up to the value reported by CRNE ranged from 1.1 to 1.8. Note that in making this re-normalization, the GME spectral slope above 95 MeV is preserved.

One other technical difficulty arises in the IMP8 data, especially in the mid 1980's: IMP8 had no on-board storage capabilities, so the data were continuously telemetered to earth. In this era, telemetry recovery was sometimes intermittent, leaving gaps in the solar-proton timelines. In most cases, these timeline-gaps can be filled reliably by simple exponential interpolations between the available measurements. In this study, these timeline-gaps were severe for only one event, 1985 April 24. We used scrubbed, but uncorrected data, from GOES5, provided by SEPEM website (<http://dev.sepem.oma.be>), to guide the temporal structure of the fill-ins in this event.

As can be seen in the various spectral plots in this paper, the proton spectra are typically double power-laws, where one power-law rolls over smoothly into an even steeper power-law. Mathematically, this form is captured by the so-called "Band function", which is smooth in both its value and first-derivative. The Band function was first introduced in the study of gamma-ray burst spectra (Band et al. 1993) and subsequently has been applied to solar particle data (Tylka et al. 2006, Tylka & Dietrich 2009, Mewaldt et al. 2005). The Band parameters needed to describe a proton spectrum are easily extracted using standard 'least-squares' minimization techniques (Tylka et al. 2006).

We show a few plots of some of the events: two each for the GLEs (Figs. 4 and 5), sub-GLEs (Figs. 6 and 7), and sub-sub GLEs (Figs. 8 and 9). Our proton spectra for GLEs that occurred between 1956-2006 have been reported in earlier work. (Tylka, et al., 2006, Tylka and Dietrich, 2008, Atwell, Tylka and Dietrich, 2008). The four Band fit parameters are shown within each plot.

**GLEs**

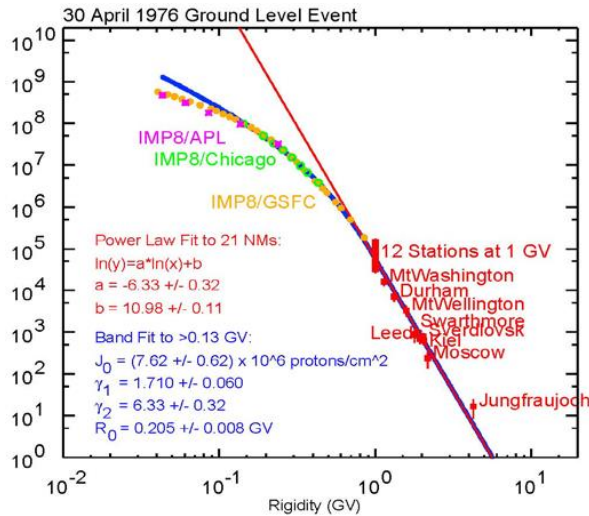


**Figure 4: Band fit for the 30 April 1976 GLE.**

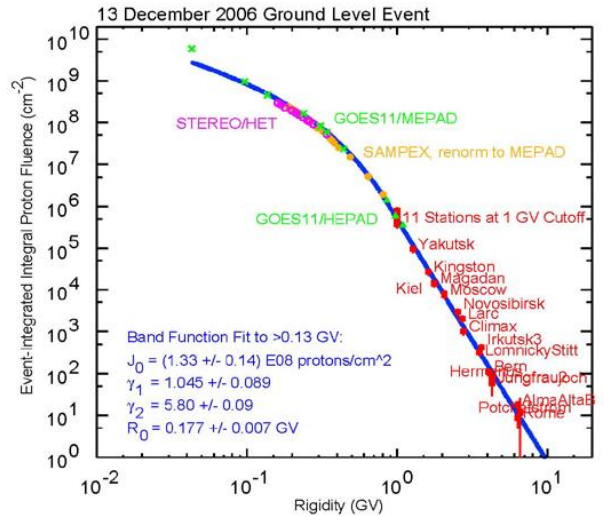


**Figure 5: Band fit for the 13 December 2006 GLE.**

**Sub-GLEs**

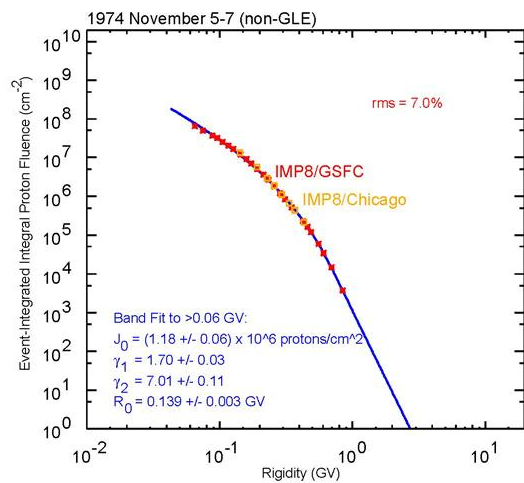


**Figure 6: Band fit for the 5 Nov 1974 sub-GLE.**

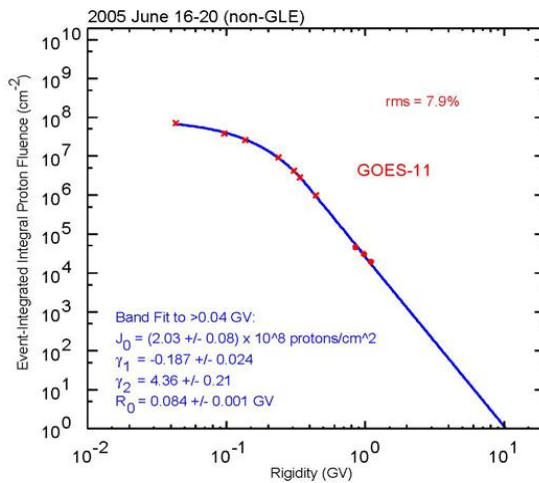


**Figure 7: Band fit for the 16 June 2005 sub-GLE.**

**Sub-sub GLEs**

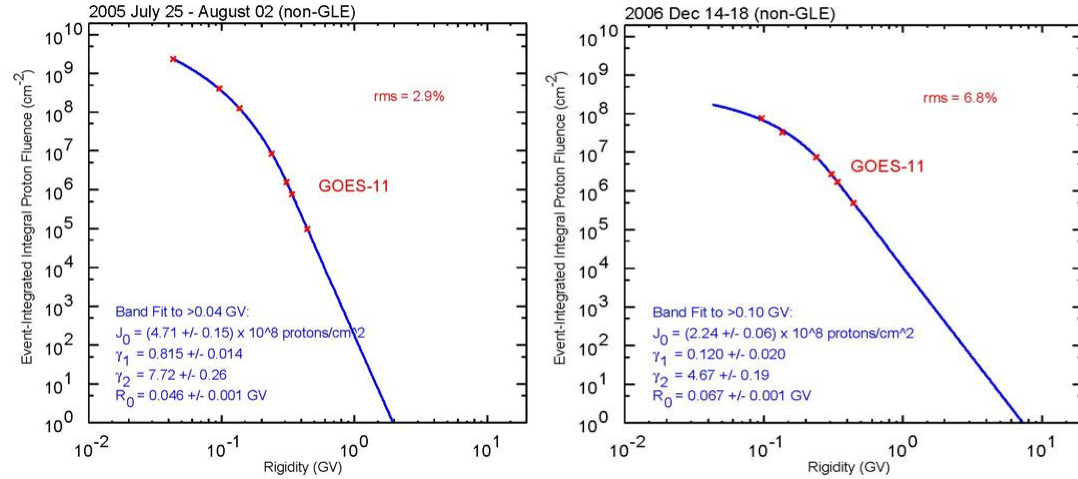


**Figure 8: Band fit for the 25 July 2005 sub-sub GLE. Figure 9: Band fit for the 14 Dec 2006 sub-sub GLE.**

It is important to note that, in general, these Band fits are valid only for proton energies greater than 10 MeV (or, equivalently, rigidities greater than 0.137 GV.) It will also be noted that a few of the Band fits have the lower-rigidity power-law index  $\gamma_1 < 0$ . Since the integral proton spectrum must be a strictly non-increasing function of rigidity, this parameter value would give unphysical results if extrapolated to very low rigidities. Nevertheless, these  $\gamma_1 < 0$  values, combined with the exponential rollover, serve to provide good empirical descriptions for the proton spectrum at energies relevant for space-system design.

#### IV. Results

The NASA Langley Research Center-developed computer code, HZETRN, a high energy particle transport/dose code, was used to make the dose computations (Townsend and Tripathi, 1995). Due to its ease of use and faster runtimes, we used the 2005 version of HZETRN for this study. Table 2 shows the absorbed dose (cGy[Si]) as a function of aluminum thickness for each event investigated. For each thickness, the highest dose is also highlighted. It is interesting to note that at small thicknesses (2 and 5 g/cm<sup>2</sup>), a sub-GLE produces more dose than a GLE.

**Table 2: Absorbed dose in various thicknesses of aluminum for SPEs during SSN < 30 (1974-2010)**

Dose, cGy(Si)



Date	Event Type	2 (g/cm <sup>2</sup> )	5 (g/cm <sup>2</sup> )	10 (g/cm <sup>2</sup> )	20 (g/cm <sup>2</sup> )	50 (g/cm <sup>2</sup> )
1976 Apr 30	GLE	4.406	1.338	0.4988	0.1656	0.029
2006 Dec 13	GLE	24.57	8.527	3.461	1.231	0.2282
1974 Nov 5	Sub-GLE	0.395	0.0994	0.0305	0.0079	0.0009
1975 Aug 21	Sub-GLE	0.0517	0.0131	0.0039	0.0009	0.0001
1975 Aug 22	Sub-GLE	0.15	0.0403	0.0123	0.0029	0.0004
1985 April 24	Sub-GLE	0.646	0.115	0.0299	0.0073	0.001
1985 Jan 22	Sub-GLE	0.193	0.0441	0.0119	0.0025	0.0002
1985 July 17	Sub-GLE	0.0786	0.0378	0.0194	0.0086	0.0021
1985 July 9	Sub-GLE	0.407	0.0952	0.0269	0.0062	0.0006
1986 Feb 14	Sub-GLE	1.84	0.306	0.0694	0.0136	0.0012
1986 Feb 6	Sub-GLE	1.48	0.47	0.178	0.0589	0.0098
1986 Feb 7	Sub-GLE	1.83	0.363	0.0947	0.0212	0.0022
1994 Oct 19	Sub-GLE	0.1932	0.0381	0.0102	0.0027	0.0003
2005 June 16	Sub-GLE	1.51	0.438	0.136	0.041	0.0079
2005 Sept 7	Sub-GLE	37.39	8.767	2.801	0.7995	0.1256
2006 Dec 6	Sub-GLE	1.25	0.26	0.07	0.02	0.004
1976 Aug 22	Sub-Sub	0.164	0.0337	0.0082	0.0016	0.0001
1986 Feb 10	Sub-Sub	0.0392	0.0104	0.0032	0.0009	0.0002
1986 Feb 16	Sub-Sub	0.103	0.0143	0.0025	0.0004	0.00004
1986 Feb 4	Sub-Sub	0.0335	0.0076	0.002	0.0005	0.0001
1986 Mar 6	Sub-Sub	0.0465	0.0075	0.0015	0.0003	0.00003
1986 May 4	Sub-Sub	0.138	0.0345	0.0099	0.0027	0.0005
2005 Aug 22	Sub-Sub	2.18	0.148	0.0181	0.0025	0.0003
2005 July 13	Sub-Sub	0.0308	0.0031	0.0005	0.0001	0.00001
2005 July 14	Sub-Sub	1.57	0.108	0.0114	0.0014	0.0002
2005 July 17	Sub-Sub	0.274	0.0323	0.0053	0.0009	0.0001
2005 July 25	Sub-Sub	1.25	0.12	0.0186	0.0029	0.0003
2005 May 13	Sub-Sub	0.302	0.0398	0.0085	0.0018	0.0002
2005 May 14	Sub-Sub	0.222	0.0147	0.0021	0.0004	0.0001
2005 Sept 1	Sub-Sub	0.0762	0.0317	0.0137	0.005	0.0013
2005 Sept 13	Sub-Sub	1.06	0.0608	0.0069	0.001	0.0002
2006 Dec 14	Sub-Sub	1.25	0.256	0.0736	0.0207	0.0036
2006 July 6	Sub-Sub	0.0462	0.0089	0.0024	0.0006	0.0001
2010 Aug 14	Sub-Sub	0.045	0.0073	0.0018	0.0004	0.0001

## V. Discussion

In reviewing the results, there are some cases where a GLE produces less absorbed dose than a sub-GLE. This is seen in the results when comparing 2005 September 7 (sub-GLE) to 2006 December 13 (GLE). At small thicknesses (2 and 5 g/cm<sup>2</sup>), the sub-GLE actually produces more dose than the GLE. However, at larger thicknesses, the GLE creates slightly more dose than the sub-GLE. Figure 10 shows a comparison of the GLEs of 1976 April 30 and 2006 December 6 and the sub-GLE 2005 September 7. At energies less than 100 MeV, there is a higher differential fluence for the sub-GLE and then after 100 MeV the 2006 December 13 GLE has a higher fluence. The 30 April 1976 GLE

has lower fluence overall when compared with the 2005 September 7 sub-GLE and thus produces a lower dose in aluminum.

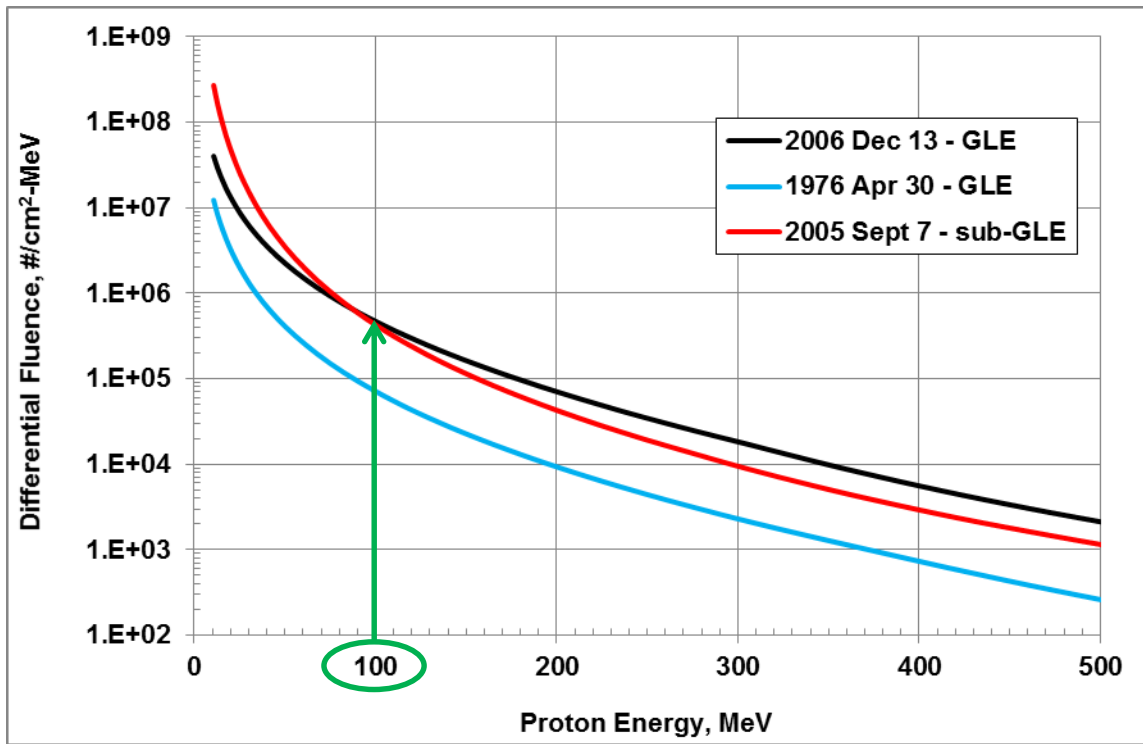
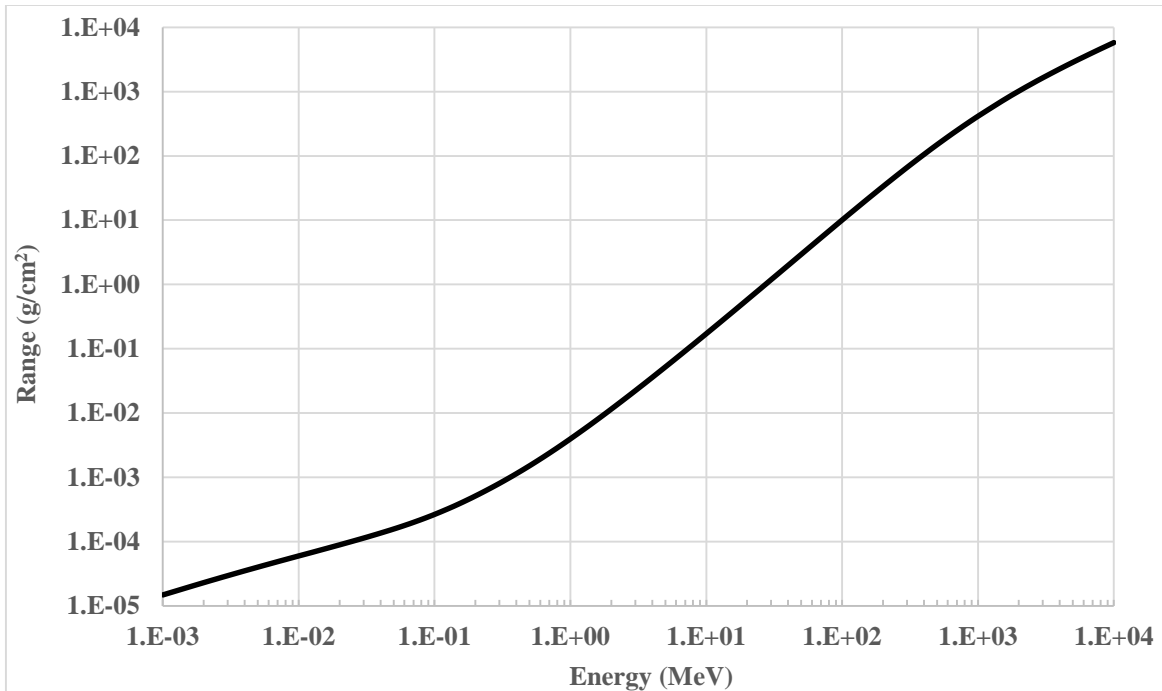


Figure 10: Comparison of the 1976 April 30 and 2006 Dec 6 GLEs and the 2005 Sept 7 sub-GLE.

The GLEs that have a high fluence of particles at high energies will not affect thinly shielded spacecraft the same as they affect more massive spacecraft. This is because the high energy particles traverse through the thinly shielded spacecraft without imparting much energy to the material. For example, if we consider the range of protons in aluminum (Figure 11), we see that particles with lower energy will be absorbed at smaller thicknesses, contributing to the dose, whereas higher energy particles require much more thickness to slow down the particle and absorb its energy. If the spacecraft is thinly shielded, these higher energy particles traverse through the spacecraft wall with minimal energy loss, and minimal dose imparted to the items within the spacecraft.



**Figure 11: Range of protons in aluminum (Berger, et al., 2009)**

Thus, the electronics within the thinly shielded spacecraft may not be as affected by the high energy particles from large SPEs. On the other hand, SPEs with a more moderate intensity can actually be more problematic for thinly shielded spacecraft, as the lower energy particles are stopped more easily by the spacecraft and internal component thicknesses. Thus, selecting the environment for the predicted solar activity of the mission timeline, as well as selecting the worst case environment for the thickness of the spacecraft, are important factors in determining the appropriate environment for the mission at hand.

This study elucidates the importance of understanding the environment under various factors: mission timeframe, mission length, spacecraft thickness, and risk capability. For smaller spacecraft with relatively thin walls (less mass overall), many of the typical worst-case SPEs used in human spaceflight will either cause the design to be more massive than necessary, or if the SPE chosen happens to be a hard spectrum, then the design may not be substantial enough to protect against the TID. Thus, it is recommended that designers consider the following when evaluating smaller spacecraft for radiation exposure.

First, the mission timeframe should be accounted for by investigating the predicted sun spot number associated with the dates of the mission. In an era of low solar-activity, it is overkill to design according to the worst-case SPEs in the historical record. Second, catalogues of proton spectra like that in Table 1 can be used to evaluate dose exposure under various depths of shielding, as shown in Table 2. Finally, with further development of comprehensive catalogues of SPE spectra during periods of low solar-activity, a probabilistic assessment of dose can be made.

## VI. Summary and Conclusions

The work evaluated in this paper is the first look at solar quiet conditions and the implications for smaller, thinner spacecraft. As a proxy for a low-level of solar activity, we focused on solar-quiet conditions where the smoothed sunspot number was less than 30. We derived the event-integrated proton spectra at energies  $>10$  MeV, which are relevant space-system designs, for all potentially significant SPEs that occurred during these months. We investigated the effect of these SPEs via absorbed dose to relatively thin spacecraft. We found that the typical worst-case scenario SPE for large, thick-walled spacecraft may not be an equivalent worst-case scenario to relatively thin spacecraft. Thus, it is important for designers to understand the solar conditions during the planned mission, as well as the spectra of SPEs corresponding to a worst-case for the spacecraft design.

## VII. Future Work

We are planning to extend this study to also include those SPEs that lie in the range of  $30 \leq \text{SSN} < 50$ . In addition, we will develop a probabilistic assessment of receiving a given dose due to these SPEs.

## References

- Atwell, W., Tylka, A., and Dietrich, W., and Francis F. Badavi, "Radiation Exposure Estimates For Extremely Large Solar Proton Events," 37th Scientific Assembly of the Committee on Space Research (COSPAR) Montreal, Canada 13-20 July 2008.
- Band, D. et al., 1993, "BATSE Observations of Gamma-Ray Burst Spectra. I – Spectral Diversity", *Astrophysical Journal* 413, 281-292.
- Berger, M.J., Coursey, J.S., Zucker, M.A., & Chang, J., "Stopping-power and range tables for electrons, protons, and helium ions," NIST, <http://www.nist.gov/pml/data/star/>.
- Garcia-Munoz, M., Mason, G.M. & Simpson, J.A., 1975, "The isotopic composition of galactic cosmic-ray lithium, beryllium, and boron", *Astrophysical Journal*, 201, L145-L148.
- Krimigis, S.M., Armstrong, T.A., & Kohl, J.W., 1973, "Measurements of the Quiet-Time Low Energy Proton, Alpha, and M-Nuclei Component in Cosmic Rays, Proceedings of the 13<sup>th</sup> International Conference on Cosmic Rays (Denver), 2, 1656-1661.
- McGuire, R.E., von Roseninge, T.T., & McDonald, F.B., 1986, "The Composition of Solar Energetic Particles", *Astrophysical Journal*, 301, 938-961.
- Mewaldt, R.A., et al., 2005, "Proton, Helium, and Electron Spectra during the Large Solar Particle Events of October-November 2003, *Journal of Geophysical Research*, 110, CITEID A09S18.
- Novikova, E.I., Dietrich, W.F., Tylka, A.J., Collins, J., and Philips, B.F., 2010, "Monte Carlo Calibration of the Response of the University of Chicago's Cosmic Ray Nuclei Experiment (CRNE) on IMP-8 to Electrons above 0.5 MeV", *Advances in Space Research*, 46, 31-43.
- Onsager T.G., et al., 1996, "Operational Uses of the GOES Energetic Particle Detectors", in *GOES-8 and Beyond*, Proc. SPIE, 2812, 281-290.
- Rodriguez, J.V., Onsager, T.G., and Mazur, J.E., 2010, "The East-West Effect in Solar Proton Flux Measurements in Geostationary Orbit: A New GOES Capability", *Geophysical Research Letters*, 37, L07109.
- Sauer, H.H., 1993 "GOES Observations of Energetic Protons to  $E > 685$  MeV: Description and Data Comparison", Proceedings of the 23<sup>rd</sup> International Cosmic Ray Conference (Calgary) 3, 250-253 and references therein.
- Sauer, H.H., undated, "NGDC Internal Technical Note on GOES Geometric Factors".
- Smart, D.F., & Shea, M.A., 1999, "Comment on the Use of GOES Solar Proton Data and Spectra in Solar Proton Dose Calculations", *Radiation Measurements*, 30, 327-335.
- Townsend, Lawrence W., & Tripathi, Ram K., "Description of a Free-Space Ion and Nucleon Transport and Shielding Computer Program, NASA Langley Research Center, Hampton, VA, NASA-TP-349, 1995.
- Tylka, A.J. & Dietrich, W.F., 1999, "IMP-8 Observations of the Spectra, Composition, and Variability of Solar Heavy Ions at High Energies Relevant to Manned Space Missions", *Radiation Measurements* 30, 345-359.
- Tylka, A.J. & Dietrich, W.F., 2009, "A New and Comprehensive Analysis of Proton Spectra in Ground Level Enhanced (GLE) Solar Particle Events", Proceedings of the 31<sup>st</sup> International Cosmic Ray Conference (Lodz), <http://icrc2009.uni.lodz.pl/proc/pdf/icrc0273.pdf>
- Tylka, A.J. & Dietrich, W.F., 2010, "Ground-Level Enhanced (GLE) Solar Particle Events at Solar Minimum", SOHO-23: Understanding a Peculiar Solar Minimum, ASP Conference Series 428, 329-334.
- Tylka, A.J., et al., 2006, "A Comparative Study of Ion Characteristics in the Large Gradual Solar Energetic Particle Events of 2002 April 21 and 2002 August 24", *Astrophysical Journal Supplement Series*, 164, 536-551.
- Tylka, A., and Dietrich, W., "Proton spectra in ground-level enhanced (GLE) solar particle events," 37th Scientific Assembly of the Committee on Space Research (COSPAR) Montreal, Canada 13-20 July 2008.